

Network-based Geometry-Free Three Carrier Ambiguity Resolution and Phase Bias Calibration

Yanming Feng, Queensland University of Technology, Australia
Chris Rizos, The University of New South Wales, Australia

Abstract

Continuously operating reference stations (CORS) are increasingly used to deliver real-time and near-real-time precise positioning services on a regional basis. A CORS network-based data processing system depends on two types of measurements: (1) ambiguity-resolved double-differenced (DD) phase measurements, and (2) phase bias calibrated zero-differenced (ZD) phase measurements. This paper describes generalized, network-based geometry-free models for three carrier ambiguity resolution (TCAR) and phase bias estimation for DD and ZD code and phase measurements. Firstly, the geometry-free TCAR models are constructed with two Extra-Widelane (EWL) and/or Widelane (WL) virtual signals to allow for rapid ambiguity resolution (AR) for DD phase measurements without distance constraints. With an ambiguity-resolved WL phase measurement and the ionospheric estimate derived from the two EWL signals, an additional geometry-free equation is formed for the third virtual signal independent of the previous two. AR with the third geometry-free model requires a longer period for averaging than the first two, but is also distance-independent. A more general formulation of the geometry-free model for a baseline or network is also introduced, where all the DD ambiguities can be more rigorously resolved using the LAMBDA method. Secondly, the geometry-free models for calibration of three carrier phase biases of ZD phase measurements are similarly defined for selected virtual signals. A network adjustment procedure is then used to improve the ZD phase biases with known DD integer constraints. Numerical results from experiments with 24-hour dual-frequency GPS data from three US CORS stations baseline lengths of 21km, 56km and 74km confirm the theoretical predictions concerning AR reliability of the network-based geometry-free algorithms.

Keywords: GNSS, Three Carrier Ambiguity Resolution, Phase Bias Calibration, Network adjustment.

1. Introduction

Continuously operating reference stations (CORS) are increasingly used to deliver real-time or near-real-time precise positioning services on a regional basis. Such an evolution from post-processed applications to real-time operations has been made possible by Internet communications between GNSS CORS, now numbering in the tens to hundreds of stations per network. Such networks are available mostly in developed areas with high population densities, and excellent Internet and mobile communications infrastructure. The SunPOZ real-time GPS services is, however, currently limited to south east Queensland (Cislowski & Higgins, 2006), as other inhibited areas with lower population densities have not been covered due to economic constraints.

A real-time CORS network, together with precise real-time GNSS orbit information available from International GNSS Service (IGS), can potentially support many types of services and applications including: network-based Real-Time Kinematic (Network-RTK) positioning, satellite Clock Determination (CD), Precise Point Positioning (PPP), Regional Integrity Determination (RID), Zenith

Tropospheric Delay (ZTD) or water vapour (WV) estimation, and ionospheric Total Electron Content (TEC) mapping. Two fundamental techniques for the realisation of the above technical capabilities are: (1) efficient and reliable ambiguity resolution of double-differenced (DD) phase measurements over long distances, such as hundreds, instead of tens, of kilometres; and (2) precise estimation/calibration of the phase biases of zero-differenced (ZD) phase measurement over much shorter periods of observations, e.g. a few minutes instead of tens of minutes. The key limitation of existing dual-frequency ambiguity resolution (AR) are the constrained service distances between reference stations and user receivers due to the impact of distance-dependent biases such as orbit error, and ionospheric and tropospheric signal delay. This has restricted the reference-user receiver distance to about 20km or less in the single-base RTK case (Rizos & Han, 2003). In current network-RTK implementations, the inter-station distance is typically 70km to 90km. Nevertheless, if the coverage of the SunPOZ network were extended to the whole inhabited area of the state of Queensland at this density, the number of CORS would reach a few hundreds, representing millions of dollars in installation costs, and significant annual operations costs.

The ZD phase ambiguity biases can be estimated by averaging a span of observations. For ionosphere-free or ionosphere-corrected measurements this averaging process is equivalent to the carrier phase smoothing of the respective code measurements over the same time span. The problem is that due to temporal correlation and the effects of multipath errors on code measurements, an averaging or smoothing time of up to tens of minutes may be required to achieve centimetre-level ranging accuracy.. In some cases, where severe systematic errors are present for a long time, an unbiased estimate can not be obtained.

Use of multiple-frequency GNSS signals could possibly redefine future RTK services on both a regional and global basis (see, e.g., Feng & Rizos, 2005; Feng, 2008; Hatch, 2006). The future GNSS services could realise regional scale network-based RTK services at the cm-dm accuracy level. The reference stations equipped with triple-frequency GNSS receivers may be spaced up to a few hundred kilometres apart, to provide differential and RTK services in regional and rural areas such as Queensland. In such low density networks, network-based ionosphere corrections may be provided to support dual-frequency users within the network coverage area, while the tropospheric corrections must be provided to support both dual- and triple-frequency users.

The concept of Three Carrier Ambiguity Resolution (TCAR) was first described in the earlier studies by Forssell et al (1997) and Vollath et al (1998). De Jonge et al (2000) and Hatch et al (2000) proposed the Cascade Integer Resolution (CIR) method. Both early TCAR and CIR use essentially the same geometry-free bootstrapping procedure. Han & Rizos (1999) proposed a geometry-free procedure resolving three virtual signals without distance constraints. In more recent efforts by Feng & Rizos (2005), Feng & Moody (2006), Hatch (2006) and Vollath (2004), the concepts and algorithms of TCAR or Multiple Carrier Ambiguity Resolution (MCAR) were proposed for use with geometry-based models as well. Feng (2008) outlined a general geometry-based modeling strategy for improved AR and positioning estimation (PE) using three or more phase and code signals. Given three L-band frequencies, the proposed strategy can generally identify the three best virtual signals to allow for more reliable AR under certain observational conditions - influenced by the magnitudes of ionospheric activity, tropospheric conditions, phase noise and orbital error. The selected virtual signals often have minimum or low ionosphere-effect, and are thus known as ionosphere-reduced virtual signals. As a

result the ionospheric effects in the geometry-based observation models are ignorable for ambiguity resolution over distances of tens to hundreds of kilometers in length.

This paper describes a more general geometry-free model for TCAR and phase bias estimation with DD and ZD code and phase measurements for network-based data processing. In the network-RTK case, the required AR performance at the network centre is different from the AR performance requirement at the user end. The network processing software can make use of the continuous recording data for the AR process and the constraints of known station coordinates, and then determine the tropospheric delays with ambiguity-resolved ionosphere-free phase measurements. In the user-based processing, ideally, the ambiguities can be fixed epoch-by-epoch with the measurements from a single epoch, or as few epochs as possible, and the accurately known tropospheric corrections. This work focuses on a network-based geometry-free TCAR modelling and network adjustment procedure to determine DD integer ambiguities and to estimate ZD phase biases. This is because when the DD integer ambiguities between multiple stations are resolved and fixed, constraints can be imposed on ZD measurements from all the stations to improve the ZD phase bias of each receiver over a short span of observations. On the other hand, precisely calibrated phase biases from previous epochs can directly form DD integers to verify the current DD solutions.

This paper is organised as follows. Section 2 introduces the general modelling strategy to search for the best virtual signals for the geometry-free TCAR. Section 3 describes the phase bias estimation algorithms in the context of three GNSS carrier signals. Section 4 provides numerical analyses performed to demonstrate the performance benefits of some of the key algorithms proposed in this paper. The final section is a summary of the findings of the paper.

2. Geometry-free TCAR models

2.1 Basic equations and definitions

To begin with, we define the observation equations for the virtual phase and code measurements in metres:

$$\begin{aligned} \phi_{(i,j,k)} = & \rho + \delta_{\text{orbit}} + c(\delta t_S - \delta t_R) + \delta_{\text{trop}} - \beta_{(i,j,k)} \frac{K_1}{f_1^2} \\ & - \lambda_{(i,j,k)} [\phi_S^0 - \phi_R^0 + N_{(i,j,k)}]_{(i,j,k)} + \varepsilon_{\phi(i,j,k)} \end{aligned} \quad (1)$$

and

$$P_{(l,m,n)} = \rho + \delta_{\text{orbit}} + c(\delta t_S - \delta t_R) + \delta_{\text{trop}} + \beta_{(l,m,n)} \frac{K_1}{f_1^2} + \varepsilon_{P(l,m,n)} \quad (2)$$

where $\phi_{(i,j,k)}$ is a linear combination of three fundamental signals (Feng & Rizos, 2005; Feng, 2008):

$$\phi_{(i,j,k)} = \frac{i \cdot f_1 \cdot \phi_1 + j \cdot f_2 \cdot \phi_2 + k \cdot f_5 \cdot \phi_5}{i \cdot f_1 + j \cdot f_2 + k \cdot f_5} \quad (3)$$

where (i, j, k) are integer coefficients; ϕ_i is the phase measurements in metres and f_i is the frequency on L_i carrier for $i=1,2$, and 5; (l, m, n) are also integer coefficients. P_1 , P_2 and P_5 are the code measurements on each of the three signals; $P_{(l,m,n)}$ is similarly defined as:

$$P_{(l,m,n)} = \frac{l \cdot f_1 \cdot P_1 + m \cdot f_2 \cdot P_2 + n \cdot f_5 \cdot P_5}{l \cdot f_1 + m \cdot f_2 + n \cdot f_5} \quad (4)$$

In both Eqs (1) and (2), ρ is the geometric distance between satellite S and receiver antenna R; c is the speed of EMR in vacuum; δ_{orbit} is the satellite orbital error in metres; δt_{R} is the receiver clock error of all components in seconds; δt_{S} is the satellite clock error of all components in seconds; δ_{trop} is the tropospheric propagation delay in metres; φ_{S}^0 is the initial phase of the satellite oscillator in cycles, which is satellite-dependent; $\frac{K_1}{f_1^2}$ is the ionospheric propagation delay with respect to L_1 phase; φ_{R}^0 is initial phase of the oscillator in cycles, which is receiver-dependent; and $\beta_{(i,j,k)}$ is the first-order ionospheric scale factor (ISF) expressed as:

$$\beta_{(i,j,k)} = \frac{f_1^2(i/f_1 + j/f_2 + k/f_5)}{i \cdot f_1 + j \cdot f_2 + k \cdot f_5} \quad (5)$$

The linearly combined signal (Eq (3)) has the virtual frequency:

$$f_{(i,j,k)} = i \cdot f_1 + j \cdot f_2 + k \cdot f_5, \quad (6)$$

the virtual wavelength:

$$\lambda_{(i,j,k)} = \frac{c}{f_{(i,j,k)}} \quad (7)$$

and the cycle ambiguity:

$$N_{(i,j,k)} = i \cdot N_1 + j \cdot N_2 + k \cdot N_5 \quad (8)$$

With any three GNSS signals, we will assume the conditions for frequencies: $f_1 > f_2 > f_5$ and $f_2 - f_5 < f_1 - f_2$.

The double-differenced (DD) phase and code measurements are:

$$\begin{aligned} \Delta \nabla \phi_{(i,j,k)} = & \Delta \nabla \rho + \Delta \nabla \delta_{\text{orbit}} + \Delta \nabla \delta_{\text{trop}} - \beta_{(i,j,k)} \frac{\Delta \nabla K_1}{f_1^2} \\ & - \lambda_{(i,j,k)} \Delta \nabla N_{(i,j,k)} + \varepsilon_{\Delta \nabla \phi(i,j,k)} \end{aligned} \quad (9)$$

and

$$\Delta \nabla P_{(l,m,n)} = \Delta \nabla \rho + \Delta \nabla \delta_{\text{orbit}} + \Delta \nabla \delta_{\text{trop}} + \beta_{(l,m,n)} \frac{\Delta \nabla K_1}{f_1^2} + \varepsilon_{\Delta \nabla P(l,m,n)} \quad (10)$$

where the symbol “ $\Delta \nabla$ ” represents the DD operation applied to the quantity immediately to the right; $\Delta \nabla \rho$ is the theoretical value of the DD range.

2.2 General formation of geometry-free TCAR models

Geometry-free TCAR directly estimates the float ambiguity parameters from virtual measurements or virtual ambiguity-fixed phase measurements. Using a virtual code measurement, the geometry-free observational model for a virtual integer parameter is generally expressed as (Feng et al, 2007):

$$\frac{\Delta \nabla P_{(l,m,n)} - \Delta \nabla \phi_{(i,j,k)}}{\lambda_{(i,j,k)}} = \Delta \nabla N_{(i,j,k)} + \frac{1}{\lambda_{(i,j,k)}} \{ [\beta_{(l,m,n)} + \beta_{(i,j,k)}] \frac{\Delta \nabla K_1}{f_1^2} + \varepsilon_{\Delta \nabla P(l,m,n)} + \varepsilon_{\Delta \nabla \phi(i,j,k)} \} \quad (11)$$

In Eq (11), (l, m, n) and (i, j, k) generally are different sets of integer values, representing various possible combinations between them.. Code and phase signals that are minimally affected by the joint ionospheric term, code and phase noises, with respect to their virtual wavelengths, should be considered the better choices for AR purposes. Three traditional choices are the WLs $(\Delta\nabla P_{(1,1,0)} - \Delta\nabla\phi_{(1,-1,0)})$ and $(\Delta\nabla P_{(1,0,1)} - \Delta\nabla\phi_{(1,0,-1)})$, as well as EWL $(\Delta\nabla P_{(0,1,1)} - \Delta\nabla\phi_{(0,1,-1)})$, where the ionospheric term in Eq (11) cancels, and the effects of the code noise term are nearly at a minimum. However, it is possible to find more useful signals for AR purpose under different ionospheric and noise conditions. Having defined a set of error budgets in Eq (11) and an appropriate choice of a virtual code measurement, e.g. $\Delta\nabla P_{(1,1,0)}$, one can identify the two most useful and linearly independent EWL/WL virtual signals. As shown in Appendix A (Feng et al, 2007), the first one is always the EWL $\phi_{(0, 1,-1)}$, which has the minimum total noise level. In each GNSS three-frequency processing procedure there are a few more EWL/WL virtual signals for the second signal choices, that is, $\phi_{(1, -4,3)}$ or $\phi_{(1, -3,2)}$, having the next lowest total noise level. Therefore, one of the two signals should be chosen as the second EWL/WL for AR. It is important to note that in the case of the traditional WL signal, $\phi_{(1, -1, 0)}$ and $\phi_{(1, 0,-1)}$ often have higher total noise levels, but remain unchanged with the different ionospheric biases. One can choose to determine the ambiguity for any one of the lower TNL signals along with the first EWL signal through a rounding process. In general, the first ambiguity is determined as:

$$\Delta\nabla N_{(0,-1,1)} = \left\lfloor \frac{\Delta\nabla P_{(1,1,0)} - \Delta\nabla\phi_{(0,1,-1)}}{\lambda_{(0,1,-1)}} \right\rfloor_{\text{round-off}} \quad (12)$$

and, the second EWL/WL signal, for instance $\phi_{(1, -3,2)}$, may be determined from:

$$\Delta\nabla N_{(1,-3,2)} = \left\lfloor \frac{\Delta\nabla P_{(1,1,0)} - \Delta\nabla\phi_{(1,-3,2)}}{\lambda_{(1,-3,2)}} \right\rfloor_{\text{round-off}} \quad (13)$$

After the first two EWL/WL signals are resolved, it is time to estimate the ionospheric bias (Feng and Rizos, 2005; Feng, 2008). The formula with the two WLs is given as follows:

$$\frac{\Delta\nabla\hat{K}_1}{f_1^2} = \frac{f_2 f_5}{f_1(f_2 - f_5)} [(\Delta\nabla\phi_{(1,0,-1)} + \lambda_{(1,0,-1)}\Delta\nabla N_{(1,0,-1)}) - (\Delta\nabla\phi_{(1,-1,0)} + \lambda_{(1,-1,0)}\Delta\nabla N_{(1,-1,0)})] \quad (14)$$

This ionospheric term is much noisier, but available autonomously at the triple-frequency user receiver. Similarly, smoothing of the above ionospheric estimation is possible.

The third virtual signal can be chosen from a new category, of which any combination is linearly independent of the previous two EWL/WL virtual signals. The problem is that there are no EWL signal candidates in the new category that allow the ambiguities to be fixed as easily as the first two signals using virtual code measurements. However, it is possible to use an ambiguity-resolved phase signal, $\phi_{(1,m,n)}$, such as $\phi_{(1,-1,0)}$, derived from the above EWL/WL category to estimate the ambiguity of the new signal, generally with the following equation:

$$\frac{\Delta\nabla\phi_{(1,-1,0)} + \lambda_{(1,-1,0)}\Delta\nabla\tilde{N}_{(1,-1,0)} - \Delta\nabla\phi_{(i,j,k)} - [\beta_{(1,-1,0)} - \beta_{(i,j,k)}] \frac{\Delta\nabla\hat{K}}{f_1^2}}{\lambda_{(i,j,k)}} = \Delta\nabla N_{(i,j,k)} + \frac{1}{\lambda_{(i,j,k)}} \{-\beta_{(1,-1,0)} + \beta_{(i,j,k)}\} \epsilon_{\left(\frac{\Delta\nabla\hat{K}}{f_1^2}\right)} + \epsilon_{\nabla\Delta\phi(1,-1,0)} - \epsilon_{\Delta\nabla(i,j,k)} \quad (15)$$

Considering the error correlations between the last three noise terms one can similarly compute the total noise levels (in units of cycles) to identify the most useful signal for AR purposes. However, unlike the selection of EWL/WL signals in the previous category where a few signals have apparently the lowest total noise level, there are hundreds of candidates, including the three original signals, $\phi_{(1,0,0)}$, $\phi_{(0,1,0)}$ or $\phi_{(0,0,1)}$ that have the same total noise level (in units of cycles). We simply chose the L1 phase measurement as the third virtual signal, whose ambiguity is determined by averaging over K epochs (Feng and Rizos, 2005):

$$\Delta\nabla N_{(1,0,0)} = \left\lfloor \frac{1}{K} \sum_{i=1}^K \frac{\Delta\nabla\phi_{(1,-1,0)} + \lambda_{(1,-1,0)}\Delta\nabla\tilde{N}_{(1,-1,0)} - \Delta\nabla\phi_{(1,0,0)} + 2.2833\frac{\Delta\nabla\hat{K}_1}{f_1^2}}{\lambda_{(1,0,0)}} \right\rfloor_{\text{round-off}} \quad (16)$$

Application of the ionospheric-refraction correction in Eq (16) removes distance dependence, but introduces a large random noise term. As a result, the ambiguity resolution of the third signal takes a longer span of measurements, theoretically, several to ten minutes or so, to correctly fix the integer ambiguity values. For a CORS network, the network-based processing software can make good use of the continuous recording of data for AR solutions. The above AR process is a feasible procedure. However, it is important to note that other virtual signals, having lower or higher wavelength than $\phi_{(1,-1,0)}$ may be also used in Eq (16). This implies that the whole AR process comprising steps Eqs (12), (13) and (16) is different from the traditional cascade integer resolution (CIR) procedure. Here we must recognize the importance of the ionospheric correction term in Eq (16), that removes or reduces the distance dependence. This feature is preferred, as it would reshape all the CORS-based applications as mentioned in the introduction section: POD, PPP, ZTD, RID and TEC estimations.

2.3 Geometry-free TCAR models for LAMBDA integer estimation

The traditional rounding method is efficient for the floating ambiguity solutions obtained from Eqs (11) and (15), which are performed separately. More generally, one can formulate the geometry-free TCAR problem as a linear observation equation:

$$L_{dd} = A\Delta\nabla N + C\Delta\nabla\delta I + \varepsilon \quad (17)$$

where for each DD, L_{dd} is the 3-by-1 observable vector, $\Delta\nabla N$ is the 3-by-1 ambiguity vector, and $\Delta\nabla\delta I$ represent the ionosphere bias term $\frac{\Delta\nabla K_1}{f_1^2}$ on the L1 phase measurement.

$$L_{dd} = \begin{bmatrix} \Delta\nabla P_{(1,1,0)} - \Delta\nabla\phi_{(1,-1,0)} \\ \Delta\nabla P_{(0,1,1)} - \Delta\nabla\phi_{(0,1,-1)} \\ \Delta\nabla\phi_{(1,-1,0)} + \lambda_{(1,-1,0)}\Delta\nabla N_{(1,-1,0)} - \Delta\nabla\phi_{(1,0,0)} \end{bmatrix}, \quad \Delta\nabla N = \begin{bmatrix} \Delta\nabla N_{(1,-1,0)} \\ \Delta\nabla N_{(0,1,-1)} \\ \Delta\nabla N_{(1,0,0)} \end{bmatrix} \quad (17a)$$

$$A = \begin{bmatrix} \lambda_{(1,-1,0)} & 0 & 0 \\ 0 & \lambda_{(0,1,-1)} & 0 \\ 0 & 0 & \lambda_{(1,0,0)} \end{bmatrix}, \quad C = \begin{bmatrix} 0 \\ 0 \\ -\beta_{(1,-1,0)} + \beta_{(1,0,0)} \end{bmatrix}, \quad \varepsilon = \begin{bmatrix} \varepsilon_{\Delta\nabla P_{(1,1,0)}} \\ \varepsilon_{\Delta\nabla P_{(0,1,1)}} \\ \varepsilon_{\Delta\nabla\phi_{(1,-1,0)}} \end{bmatrix} - \begin{bmatrix} \varepsilon_{\Delta\nabla\phi_{(1,-1,0)}} \\ \varepsilon_{\Delta\nabla\phi_{(0,1,-1)}} \\ \varepsilon_{\Delta\nabla\phi_{(1,0,0)}} \end{bmatrix}$$

In the dual-frequency case, the above notation L_{dd} represents the 2-by-1 observable vector for each DD

measurement; and $\Delta\nabla\mathbf{N}$ is the 2-by-1 ambiguity vector.

$$\begin{aligned} \mathbf{L}_{dd} &= \begin{bmatrix} \Delta\nabla\mathbf{P}_{(1,1)} - \Delta\nabla\phi_{(1,-1)} \\ \Delta\nabla\phi_{(1,-1)} + \Delta\nabla\tilde{\mathbf{N}}_{(1,-1)} - \Delta\nabla\phi_{(4,-3)} \end{bmatrix}, \quad \Delta\nabla\mathbf{N} = \begin{bmatrix} \Delta\nabla\mathbf{N}_{(1,-1)} \\ \Delta\nabla\mathbf{N}_{(4,-3)} \end{bmatrix} \\ \mathbf{A} &= \begin{bmatrix} \lambda_{(1,-1)} & 0 \\ 0 & \lambda_{(4,-3)} \end{bmatrix}, \quad \mathbf{C} = \begin{bmatrix} 0 \\ -\beta_{(1,-1)} + \beta_{(4,-3)} \end{bmatrix}, \quad \boldsymbol{\varepsilon}_{dd} = \begin{bmatrix} \boldsymbol{\varepsilon}_{\Delta\nabla\mathbf{P}_{(1,1)}} - \boldsymbol{\varepsilon}_{\Delta\nabla\phi_{(1,-1)}} \\ \boldsymbol{\varepsilon}_{\Delta\nabla\phi_{(1,1)}} - \boldsymbol{\varepsilon}_{\Delta\nabla\phi_{(4,-3)}} \end{bmatrix} \end{aligned} \quad (17b)$$

For a network numbering n stations with m satellites in common view, there will be M sets of DD measurements, where $M=(n-1)(m-1)$. One can regard Eq (16) as an overall linear equation, where, for instance, for the three frequencies, \mathbf{L}_{dd} is the $3M$ -by-1 observable vector; $\Delta\nabla\mathbf{N}$ is the $3M$ -by-1 integer vector, \mathbf{A} is a $3M$ -by- $3M$ constant matrix, \mathbf{C} is a $3M$ -by- M matrix, $\Delta\nabla\mathbf{N} \delta\tilde{\mathbf{I}}$ is the M -by-1 ionosphere-bias vector, and $\boldsymbol{\varepsilon}_{dd}$ is the $3M$ -by-1 total noise vector.

Given the a priori ionospheric bias $\Delta\nabla\delta\tilde{\mathbf{I}}$ with the variance-covariance (vc-) matrix $\mathbf{Q}_{\Delta\nabla\delta\tilde{\mathbf{I}}}$ and the vc-matrix for the total noise vector $\boldsymbol{\varepsilon}$, \mathbf{Q}_{dd} , which considers the geometry-dependence and variance variations between all the virtual DD measurements on a baseline or network basis, the least squares solution of Eq (16) would be:

$$\begin{bmatrix} \Delta\nabla\hat{\mathbf{N}} \\ \hat{\boldsymbol{\delta}}_{\Delta\nabla\delta\tilde{\mathbf{I}}} \end{bmatrix} = \begin{bmatrix} \mathbf{A}^T \mathbf{Q}_{dd}^{-1} \mathbf{A} & \mathbf{A}^T \mathbf{Q}_{dd}^{-1} \mathbf{C} \\ \mathbf{C}^T \mathbf{Q}_{dd}^{-1} \mathbf{A} & \mathbf{C}^T \mathbf{Q}_{dd}^{-1} \mathbf{C} + \mathbf{Q}_{\Delta\nabla\delta\tilde{\mathbf{I}}}^{-1} \end{bmatrix}^{-1} \begin{bmatrix} \mathbf{A}^T \mathbf{Q}_{dd}^{-1} (\mathbf{L}_{dd} - \mathbf{C} \Delta\nabla\delta\tilde{\mathbf{I}}) \\ \mathbf{C}^T \mathbf{Q}_{dd}^{-1} (\mathbf{L}_{dd} - \mathbf{C} \Delta\nabla\delta\tilde{\mathbf{I}}) \end{bmatrix} \quad (18)$$

To solve this problem the LAMBDA search algorithm can be used.

For each epoch there is an equation like Eq (17):

$$\mathbf{L}_{dd}(\mathbf{k}) = \mathbf{A} \Delta\nabla\mathbf{N} + \mathbf{C} \Delta\nabla\delta\tilde{\mathbf{I}}(\mathbf{k}) + \boldsymbol{\varepsilon}_{dd}(\mathbf{k}), \text{ for } \mathbf{k}=1, 2, \dots, \mathbf{K}. \quad (19)$$

With a priori ionospheric bias, $\Delta\nabla\delta\tilde{\mathbf{I}}(\mathbf{k})$, one can average over \mathbf{K} epochs to obtain a better approximation of the float ambiguity and the common ionospheric error $\hat{\boldsymbol{\delta}}_{\Delta\nabla\delta\tilde{\mathbf{I}}}$ with respect to $\delta\tilde{\mathbf{I}}(\mathbf{k})$ as follows:

$$\begin{bmatrix} \Delta\nabla\hat{\mathbf{N}} \\ \hat{\boldsymbol{\delta}}_{\Delta\nabla\delta\tilde{\mathbf{I}}} \end{bmatrix} = \left\{ \sum_{\mathbf{k}=1}^{\mathbf{K}} \begin{bmatrix} \mathbf{A}^T \mathbf{Q}_{dd}^{-1}(\mathbf{k}) \mathbf{A} & \mathbf{A}^T \mathbf{Q}_{dd}^{-1}(\mathbf{k}) \mathbf{C} \\ \mathbf{C}^T \mathbf{Q}_{dd}^{-1}(\mathbf{k}) \mathbf{A} & \mathbf{C}^T \mathbf{Q}_{dd}^{-1}(\mathbf{k}) \mathbf{C} + \mathbf{Q}_{\Delta\nabla\delta\tilde{\mathbf{I}}}^{-1}(\mathbf{k}) \end{bmatrix} \right\}^{-1} \begin{bmatrix} \sum_{\mathbf{k}=1}^{\mathbf{K}} \mathbf{A}^T \mathbf{Q}_{dd}^{-1}(\mathbf{k}) [\mathbf{L}_{dd}(\mathbf{k}) - \mathbf{C} \Delta\nabla\delta\tilde{\mathbf{I}}(\mathbf{k})] \\ \sum_{\mathbf{k}=1}^{\mathbf{K}} \mathbf{C}^T \mathbf{Q}_{dd}^{-1}(\mathbf{k}) [\mathbf{L}_{dd}(\mathbf{k}) - \mathbf{C} \Delta\nabla\delta\tilde{\mathbf{I}}(\mathbf{k})] \end{bmatrix} \quad (20)$$

If we ignore the effects of ionospheric errors of the a priori correction $\Delta\nabla\delta\tilde{\mathbf{I}}(\mathbf{k})$, the float solution of the ambiguity parameters in Eq (19) become:

$$\Delta\nabla\hat{\mathbf{N}} = \left[\sum_{\mathbf{k}=1}^{\mathbf{K}} \mathbf{A}^T \mathbf{Q}_{dd}^{-1}(\mathbf{k}) \mathbf{A} \right]^{-1} \left(\sum_{\mathbf{k}=1}^{\mathbf{K}} \mathbf{A}^T \mathbf{Q}_{dd}^{-1}(\mathbf{k}) [\mathbf{L}_{dd}(\mathbf{k}) - \mathbf{C} \Delta\nabla\delta\tilde{\mathbf{I}}(\mathbf{k})] \right) \quad (21)$$

A priori ionospheric knowledge may be obtained through interpolation of a regional or local ionospheric grid. Feng and Rizos (2007) described an alternative method which can predict the current ionospheric bias using the ionospheric estimates obtained over several previous epochs. A DD ionospheric bias on L1, $\Delta\nabla\delta I = \frac{\Delta\nabla K_1}{f_1^2}$, can be estimated using the ambiguity-fixed DD phase measurements of the L1 and L2 measurements. For each satellite-receiver pair, the prediction value $\Delta\nabla\delta\tilde{I}(k)$ at epoch t_k is based on the 1st-order or 2nd-order polynomial fit of the observed ionospheric biases over the past several to tens of epochs. The measurement L_{dd} at the current epoch t_k is then corrected with $C\Delta\nabla\delta\tilde{I}(k)$ as indicated in Eqs (20) and (21).

3. Three carrier phase-bias estimation for ZD phase measurements

With three or more GNSS frequencies, theoretically it is possible to refine the bias term in the phase measurements and estimate or reduce the effect of ionospheric delays simultaneously. Referring to Eqs (6) and (7), we may define the phase bias term in the ZD, or line-of-sight (LoS), phase measurement as (Feng et al, 2007):

$$P_{(l,m,n)} - \phi_{(i,j,k)} = \lambda_{(i,j,k)} (N + \phi_S^0 - \phi_R^0)_{(i,j,k)} - \{ [\beta_{(l,m,n)} + \beta_{(i,j,k)}] \frac{K_1}{f_1^2} + \varepsilon_{P(l,m,n)} + \varepsilon_{\phi(i,j,k)} \} \quad (22)$$

where (l, m, n) and (i, j, k) are, in general, different groups of integers. Code and phase signals with minimal effects due to ionospheric delays and code and phase noises, should be considered the best choice for the estimation of the phase bias term. However, the key problem is the ionospheric delay in the slant path ZD measurements, $\delta I_{\phi_1} = \frac{K_1}{f_1^2}$ which is of the order of metres to tens of metres. In some combinations, such as $(P_{(1,1,0)} - \phi_{(1,-1,0)})$, $(P_{(1,0,1)} - \phi_{(1,0,-1)})$, as well as $(P_{(0,1,1)} - \phi_{(0,1,-1)})$, the ionospheric term in Eq (16) cancels, and the effect of the code noise term is nearly a minimum. However, the bias-fixed phase WL $\phi_{(1,-1,0)}$ is not useful for positioning without removing the ionosphere bias. In the mean time, the ionospheric estimation with the bias-fixed phase $\phi_{(1,-1,0)}$ and $\phi_{(1,0,-1)}$ would suffer from significantly amplified uncertainty, thus not being as helpful as Eq (14). Therefore one chooses the ionosphere-free combination, for instance in the GPS case, $(P_{(77,-600)} - \phi_{(77,-600)})$, or the ionosphere-reduced NL signal $(P_{(77,-600)} - \phi_{(4,0,-3)})$ which is about four times noisier than the previous three choices, but can be directly used for positioning without further ionospheric correction. For the three chosen ZD virtual signals, the observation equations for three phase bias parameters are:

$$\begin{bmatrix} P_{(1,1,0)} - \phi_{(1,-1,0)} \\ P_{(0,1,1)} - \phi_{(0,1,-1)} \\ P_{(77,-600)} - \phi_{(4,0,-3)} \end{bmatrix} = \begin{bmatrix} \lambda_{(1,-1,0)} & 0 & 0 \\ 0 & \lambda_{(0,1,-1)} & 0 \\ 0 & 0 & \lambda_{(4,0,-3)} \end{bmatrix} \begin{bmatrix} N_{(1,-1,0)} \\ N_{(0,1,-1)} \\ N_{(4,0,-3)} \end{bmatrix} + \begin{bmatrix} \varepsilon_{P(1,1,0)} - \varepsilon_{\phi(1,-1,0)} \\ \varepsilon_{P(0,1,1)} - \varepsilon_{\phi(0,1,-1)} \\ \varepsilon_{P(77,-600)} - \varepsilon_{\phi(4,0,-3)} \end{bmatrix} \quad (23)$$

In the dual-frequency case there are two observation equations:

$$\begin{bmatrix} \mathbf{P}_{(1,1)} - \phi_{(1,-1)} \\ \mathbf{P}_{(77,-60)} - \phi_{(4,-3)} \end{bmatrix} = \begin{bmatrix} \lambda_{(1,-1)} & 0 \\ 0 & \lambda_{(4,-3)} \end{bmatrix} \begin{bmatrix} \mathbf{N}_{(1,-1)} \\ \mathbf{N}_{(4,-3)} \end{bmatrix} + \begin{bmatrix} \boldsymbol{\varepsilon}_{\mathbf{P}(1,1)} - \boldsymbol{\varepsilon}_{\phi(1,-1)} \\ \boldsymbol{\varepsilon}_{\mathbf{P}(77,-60)} - \boldsymbol{\varepsilon}_{\phi(4,-3)} \end{bmatrix} \quad (24)$$

The traditional approach is to perform simple averaging for the phase biases in Eqs (23) or (24) separately. A more rigorous approach is the least squares estimation procedure described below. At epoch k , the generalised linear equations for all n stations and m satellites are expressed as:

$$\mathbf{L}_{zd}(k) = \mathbf{B}\mathbf{N} + \boldsymbol{\varepsilon}_{zd}(k), \text{ for } k=1,2,\dots, \quad (25)$$

where \mathbf{L}_{zd} is a $3nm$ -by- 1 observational vector; \mathbf{B} is the $3nm$ -by- $3nm$ matrix; \mathbf{N} is the $3nm$ -by- 1 phase bias vector (non-integer); and $\boldsymbol{\varepsilon}_{zd}$ is $3nm$ -by- 1 total noise vector with the vc-matrix $\mathbf{Q}_{zd}(k)$. $\mathbf{Q}_{zd}(k)$ is a quasi-diagonal matrix, which reflects the correlation between the noise terms in equation (23) or (24) and the code noise levels. For instance, in the GPS L1 and L2 cases, the sub vc-matrix q_{zd} for each line-of-sight direction can be computed as follows:

$$q_{zd} = \sigma_0^2 \begin{bmatrix} 0.5620 & 0.4380 \\ 2.5457 & -1.5457 \end{bmatrix} \begin{bmatrix} \frac{\sigma_{P1}^2}{\sigma_0^2} & 0 \\ 0 & \frac{\sigma_{P2}^2}{\sigma_0^2} \end{bmatrix} \begin{bmatrix} 0.5620 & 2.5457 \\ 0.4380 & -1.5457 \end{bmatrix} \quad (26)$$

where the variance σ_0^2 is the a priori unit-weight variance. The variances for code measurements σ_{p1}^2 and σ_{p2}^2 may generally vary from epoch to epoch, depending on the multipath variations. One may choose to model them as a function of elevation of the ZD direction (see the treatment by Han, 1997, and many other investigators).

Finally, we can find the least-square estimate of equation (25) over K epochs:

$$\hat{\mathbf{N}} = \left[\sum_{k=1}^K \mathbf{B}^T \mathbf{Q}_{zd}^{-1}(k) \mathbf{B} \right]^{-1} \sum_{k=1}^K \mathbf{B}^T \mathbf{Q}_{zd}^{-1}(k) \mathbf{L}_{zd}(k) \quad (27)$$

When $K > 1$, the unit-weight variance can be estimated, for the dual-frequency case being:

$$\hat{\sigma}_0^2 = \frac{\sum_{k=1}^K (\mathbf{L}_{zd}(k) - \mathbf{B}\hat{\mathbf{N}})^T \mathbf{Q}_{zd}^{-1}(k) (\mathbf{L}_{zd}(k) - \mathbf{B}\hat{\mathbf{N}})}{2nm(K-1)} \quad (28)$$

The vc-matrix for the estimate $\hat{\mathbf{N}}$ is:

$$\mathbf{Q}_{\hat{\mathbf{N}}} = \hat{\sigma}_0^2 \left[\sum_{k=1}^K \mathbf{B}^T \mathbf{Q}_{zd}^{-1}(k) \mathbf{B} \right]^{-1} \quad (29)$$

The estimate in equation (27) theoretically gives real-valued phase biases, as defined in equation (6). But applying the double-difference operation to \mathbf{N} the satellite and receiver dependent phase biases will cancel, thus leading to DD float ambiguity solutions. Rounding these float ambiguities will produce the

solution for the DD integer vector $\Delta\mathbf{V}_N$ in equation (19). In practice, this could well be the case for the EWL or WL signals, but not for the ML/NL signals, where the effects of code noise could still be too large for correct integer resolution, despite averaging over long observation periods.

The next procedure is a network-adjustment approach which considers the DD integer constraints. If the DD integer ambiguities can be resolved, the known DD integers can be used to improve the estimates of the ZD phase biases, taking advantage of multiple stations and high quality measurements from some stations in the network. As shown in Fig 1, for 3 satellites and 3 stations we can form $(n-1)(m-1)=4$ DD measurements and $nm=9$ ZD measurements. The 4 known DD integers provided constraints between the 9 ZD phase-biases, thus improving the ZD bias estimates.

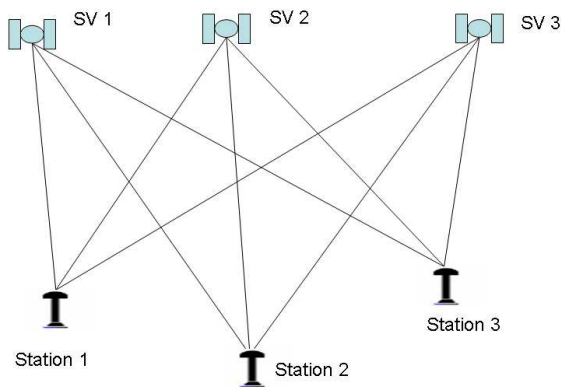


Fig 1. Geometry of 4 DD and 9 ZD measurements

In general, given the $3nm$ -by- 1 ZD phase bias vector \mathbf{Y}_N which represents the virtual observational vector from the estimated \hat{N} with the noise vector $\boldsymbol{\varepsilon}_N$, the following linear equation and statistical conditions are obtained:

$$\begin{aligned} \mathbf{Y}_N &= \mathbf{X} + \boldsymbol{\varepsilon}_N \\ E(\boldsymbol{\varepsilon}_N) &= 0, \quad \text{Cov}(\boldsymbol{\varepsilon}_N) = \mathbf{Q}_N \end{aligned} \quad (30)$$

where \mathbf{X} is the n -by- 1 phase bias vector to be re-estimated. When the DD integers are obtained for a baseline or a network of multiple stations, the following constraint equations can be introduced:

$$\mathbf{D}\mathbf{X} = \mathbf{Y}_{\Delta\mathbf{V}_N} \quad (31)$$

where \mathbf{D} is the double-difference operator matrix, and $\mathbf{Y}_{\Delta\mathbf{V}_N}$ is the known DD integer vector (which should be transferred from the known integers to match the types of phase measurements in equation (30)). The least-squares solution to equations (30) and (31) is:

$$\hat{\mathbf{X}} = \mathbf{Q}_N [\mathbf{I} - \mathbf{D}^T (\mathbf{D}\mathbf{Q}_N\mathbf{D}^T)^{-1} \mathbf{D}\mathbf{Q}_N] \mathbf{Q}_N^{-1} \mathbf{Y}_N + \mathbf{Q}_N \mathbf{D}^T (\mathbf{D}\mathbf{Q}_N\mathbf{D}^T)^{-1} \mathbf{Y}_{\Delta\mathbf{V}_N} \quad (32)$$

It is important to note that in equation (32), \mathbf{Y}_N and $\mathbf{Y}_{\Delta\mathbf{V}_N}$ must be given in the same length units.

4. Performance benefits analysis

To address the major concerns about the performance of the integer solution and phase bias solutions described in Sections 2 and 3, we will examine:

- the AR success probabilities for two EWL/WL signals over varying long baselines characterised by different levels of ionospheric biases;
- the AR success rate improvement when the network-based geometry-free TCAR is performed using the LAMBDA method compared to the direct rounding results, using dual-frequency GPS data;
- the STD improvement of the phase bias estimates obtained from the proposed network-based adjustment procedures; and
- the consistency between theoretical prediction and actual statistical results in the various solution parameters.

4.1 Performance benefits of the selected EWL/WL signals

To obtain the integer solutions from the geometry-free equations (13) and (15), the direct method is to round the observables to their nearest integers. If we assume the total noise vector ϵ_{TN} is normally distributed with zero mean and the variance σ_{TN}^2 as given in the last three columns of Appendix A, the probability of obtaining correct integers under three different sets of error budgets for double differenced code and phase measurements can be estimated:

$$P(-0.5 < \epsilon_{TN} < 0.5) = \frac{1}{\sigma_{TN}\sqrt{2\pi}} \int_{-0.5}^{+0.5} \exp\left(-\frac{x^2}{2\sigma_{TN}^2}\right) dx \quad (33)$$

Table 1. Estimated probability of AR success for the two EWL/WL signals

	$\sigma_{\delta l}=40\text{cm}$ $\sigma_{\phi 1}=1\text{cm}$ $\sigma_{P1}=60\text{cm}$		$\sigma_{\delta l}=60\text{cm}$ $\sigma_{\phi 1}=1\text{cm}$ $\sigma_{P1}=60\text{cm}$		$\sigma_{\delta l}=100\text{cm}$ $\sigma_{\phi 1}=1\text{cm}$ $\sigma_{P1}=60\text{cm}$	
	σ_{TN}	$0.5\sigma_{TN}$	σ_{TN}	$0.5\sigma_{TN}$	σ_{TN}	$0.5\sigma_{TN}$
GPS L1, L2, L5						
$\phi_{(0,1,-1)}$	100	100	100	100	100	100
$\phi_{(1,-4,3)}$	84.19	99.52	82.58	99.34	77.85	98.6
$\phi_{(1,-1,0)}$	69.11	95.80	69.11	95.80	69.11	95.80
Galileo L1, E6, E5A						
$\phi_{(0,1,-1)}$	99.76	100	99.53	100	98.26	100
$\phi_{(1,-3,2)}$	96.71	100	93.92	99.98	84.55	99.6
$\phi_{(1,-1,0)}$	76.48	98.25	76.48	98.25	76.48	98.25
Galileo L1, E6, E5B						
$\phi_{(0,1,-1)}$	100	100	99.99	100	99.93	100

$\phi_{(1,-3,2)}$	92.85	99.97	91.64	99.95	87.88	99.8
$\phi_{(1,-1,0)}$	76.48	98.25	76.48	98.25	76.48	98.25
Compass E1, E6, E5B						
$\phi_{(0,1,-1)}$	100	100	100	100	99.99	100
$\phi_{(1,-3,2)}$	89.98	99.9	87.83	99.8	81.47	99.2
$\phi_{(1,-1,0)}$	72.79	97.21	72.79	97.21	72.79	97.21
Compass E2 E6 E5B						
$\phi_{(0,1,-1)}$	100	100	100	100	99.99	100
$\phi_{(1,-3,2)}$	91.3	99.94	90.46	99.92	87.95	99.8
$\phi_{(1,-1,0)}$	77.18	98.37	77.18	98.37	77.18	98.37

Table 1 shows the probability of AR success as percentages for the two EWL/WL virtual signals in each GNSS service, with the often used WL signal for comparison. In each GNSS service defined by three frequencies, σ_{TN} takes the values of 1.0 cm and 0.5 cm (e.g., $0.5 \sigma_{TN}$), representing the total noise levels achievable with a single epoch and after averaging over several epochs, respectively. It is important to note that the rounding process of the first two EWL/WL signals consists of two independent processes for each DD set. However, the probability of the correctness of the third integer obtained by Eq (16) is conditional on the probability of the correctness of the previous two EWL/WL signals. Nevertheless, the probability of the third integers exhibits no dependence between different DD sets. In other words, the geometry-free TCAR processes described in Section 2 would by no means be a bootstrapping procedure between DD sets.

It can be generally observed that the estimates from the first best EWLs using single epoch measurements can achieve success rates of greater than 98%, which can be easily improved to 100% by averaging over several epochs. AR of the second selected EWL/WL signal does not result in AR success rates as high as the first EWL, but still performs significantly better than that of the WL signal $\phi_{(1,-1,0)}$ often used in other TCAR methods (Hatch, 2000, 2006; Feng and Rizos, 2005).

4.2 AR performance for the WL and NL signals with dual-frequency data

Four GPS data sets from 1 January 2007 were downloaded from <http://www.ngs.noaa.gov/CORS>. With a data interval of 15 seconds for the 24 hour observation spans, there are about 72562 DD phase measurements for each of the three independent baselines, as outlined in Table 2. The real AR success rate, or *AR reliability*, is defined as the ratio of the correct integers to the total number of DD phase measurements (Feng & Wang, 2007). The experiments were performed with three computing schemes for each of the three baselines:

- geometry-free rounding process for WL $\phi_{(1,-1)}$ and NL $\phi_{(4,-3)}$ phase ambiguities from measurements of a single epoch;
- geometry-free rounding process for WL $\phi_{(1,-1)}$ and NL $\phi_{(4,-3)}$ phase ambiguities from 4 epochs of measurements (one minute span); and

- geometry-free LAMBDA process for WL $\phi_{(1,-1)}$ and NL $\phi_{(4,-3)}$ phase ambiguities from measurements of a single epoch.

Table 2 summarises the actual AR success rates and total noise levels obtained using the different computing schemes for each baseline. The true DD integer solutions for WL $\phi_{(1,-1)}$ and NL $\phi_{(4,-3)}$ were obtained from geometry-based LAMBDA algorithms with an AR reliability of over 99.9%. As a result, the percentages are given in Table 1 with respect to the true integer solutions. The LAMBDA integer search starts with equation (21), where the ionospheric correction term was set to zero and the vc-matrix simply considers the geometry-dependence between the DD measurements in this context. From this table one can observe the following:

- (1) Averaging over multiple epochs apparently improves the percentage of correct integer solutions for the WL $\phi_{(1,-1)}$, but does very little for the NL $\phi_{(4,-3)}$, due to the systematic effects of the ionospheric biases in equation (16). This situation is reversed if the effects of the ionospheric term became random after corrections.
- (2) With respect to the direct rounding process, the LAMBDA procedure results in only a slight improvement of the AR success rate, if taking the geometry-dependence between DD measurements in equation (17) into consideration.
- (3) Through the rounding process, the actual AR success rate is very close to, or slightly higher than, the predicted probability from the actual statistical σ_{TN} value given in Table 1. In other words, the AR theoretical prediction using equation (31) is consistent with the actual results.

4.3 Performance benefits of ZD phase bias estimation with DD integer constraints

Four computing schemes were designed to demonstrate the performance benefits of the proposed ZD phase bias estimate equation (27) and the network-adjustment estimate in equation (32), as shown in Table 3. The statistical values of maximum (max) and minimum (min) errors, and standard deviations (STD) for ZD WL and NL phase bias estimates were based on the data of the period from GPST 00:10 to 01:33, during which all three stations tracked the same eight GPS satellites. Referring to the computing schemes I and II based on single epoch measurements, we compare the max, min values and STD values of the LoS at the site P473 to the eight satellites in Figs 2 and 3, for WL $\phi_{(1,-1)}$ and NL $\phi_{(4,-3)}$ biases respectively. Figs 4 and 5 compare STD values obtained from all four computing schemes. From these figures it is clearly observed that network-adjustment with three stations (2DD integer constraints) indeed effectively reduces the max, min and STD errors, which is especially the case for the LoS directions with the large max/min/STD errors. For instance, for the satellite PRN 16, the ZD WL bias estimate max/min/STD errors were reduced by a factor of 2 after the adjustment. Overall STD for all 3 stations and 8 satellites is improved by a factor of about 1.4. As shown in Figs 4 and 5, this improvement is equivalent to that achieved by averaging of 4 epochs. Certainly using more stations would result in more evident improvement.

Table 2. AR success rates for geometry-based and geometry-free AR solutions

Solution scenarios		Rounding	Rounding	LAMBDA
Number of epochs		1	4	1
Baseline P474- P478 21km	$\Delta\nabla N_{(1,-1)}$	74.80%	94.00%	75.00%
	$\sigma_{TN(cyc)}$	0.458	0.261	-
	$\Delta\nabla N_{(4,-3)}$	98.97	99.24%	99.35%
	$\sigma_{TN(cyc)}$	0.173	0.160	-
Baseline P473 -P378 53km	$\Delta\nabla N_{(1,-1)}$	75.39%	94.74%	75.43%
	$\sigma_{TN(cyc)}$	0.459	0.253	-
	$\Delta\nabla N_{(4,-3)}$	87.86%	87.99%	88.67%
	σ_{TN}	0.330	0.326	-
Baseline P473- P473 74km	$\Delta\nabla N_{(1,-1)}$	77.44%	95.79	77.90%
	$\sigma_{T(cyc)}$	0.4325	0.236	-
	$\Delta\nabla N_{(4,-3)}$	79.30%	79.36%	79.33%
	$\sigma_{TN(cyc)}$	0.4274	0.4252	-

To more generally demonstrate the performance benefits of the network-based phase bias estimation strategy, Fig 6 illustrates the convergence of various orders of magnitudes of the initial ZD phase bias errors (single epoch) versus the filtering time (epochs) under zero mean and white noise conditions. When the single epoch ZD phase bias error is as large as several metres it takes a long time to converge to decimetre-level ZD ranging accuracy. If the single epoch phase bias accuracy has been improved to the sub-metre level, achieving the same decimetre ZD bias accuracy would take a much shortened filtering/averaging time, and easily result in centimetre-level ZD ranging accuracy. The network-based phase bias estimation strategy provides the possibility to achieve sub-metre initial phase bias accuracy.

Table 3. Four computing schemes

Scheme	# of epochs	# of stations	Station ID	PRNs
I	1	1	P473, P478, P474	6, 29,
II	1	3		10, 26,
III	4	1		22,7,21
IV	4	3		

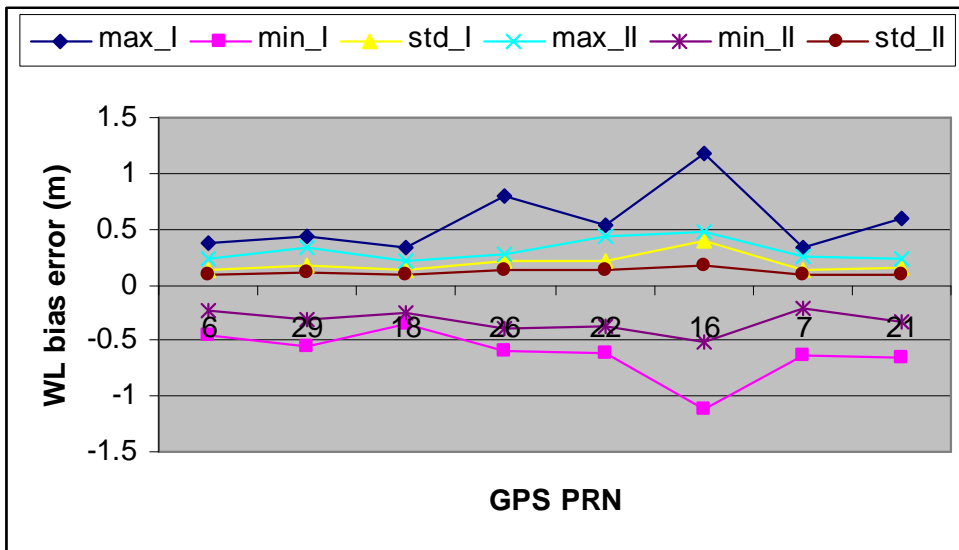


Fig 2. Comparison of max, min and STD values of the WL $\phi_{(1,-1)}$ phase bias estimation errors with computing schemes I and II based on single epoch measurements, showing apparent improvement through the network adjustment process with DD integer constraints.

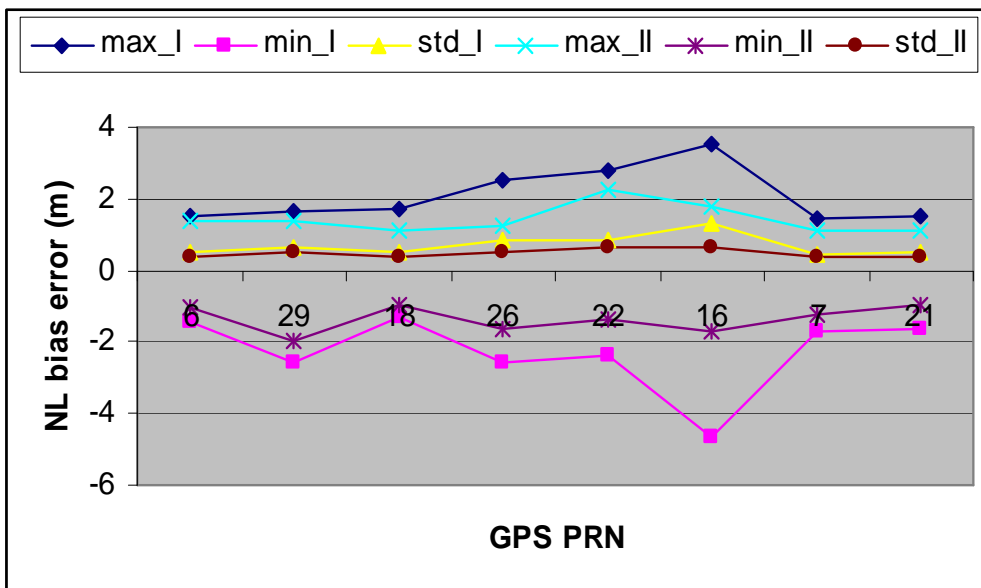


Fig 3. Comparison of max, min and STD values of the NL $\phi_{(4,-3)}$ phase bias estimation errors of computing schemes I (1 epoch and 1 station), II (1 epoch, 3 stations), showing apparent improvement via the network adjustment procedure with DD integer constraints.

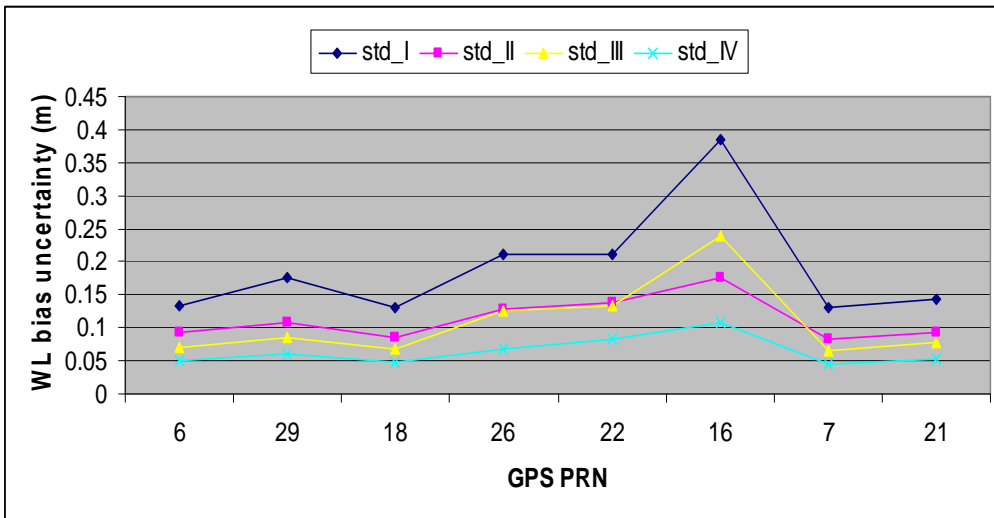


Fig 4. STD values of the WL $\phi_{(1,-1)}$ phase bias estimation errors between all computing schemes I (1 epoch and 1 station), II (1 epoch, 3 stations), III (4 epochs, 1 station) and IV (4 epochs, 3 stations). The overall STD is reduced to a factor of 1.4 through network adjustment with 2 DD integer constraints.

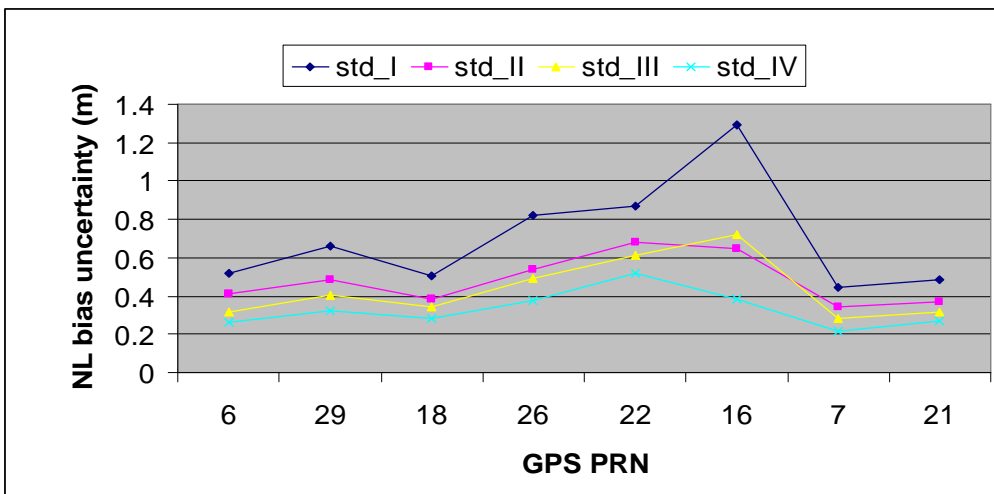


Fig 5. STD values of the NL $\phi_{(4,-3)}$ phase bias estimation errors between all computing schemes I (1 epoch and 1 station), II (1 epoch, 3 stations), III (4 epochs, 1 station) and IV (4 epochs, 3 stations). The overall STD is reduced to a factor of 1.4 through network adjustment with 2 DD integer constraints.

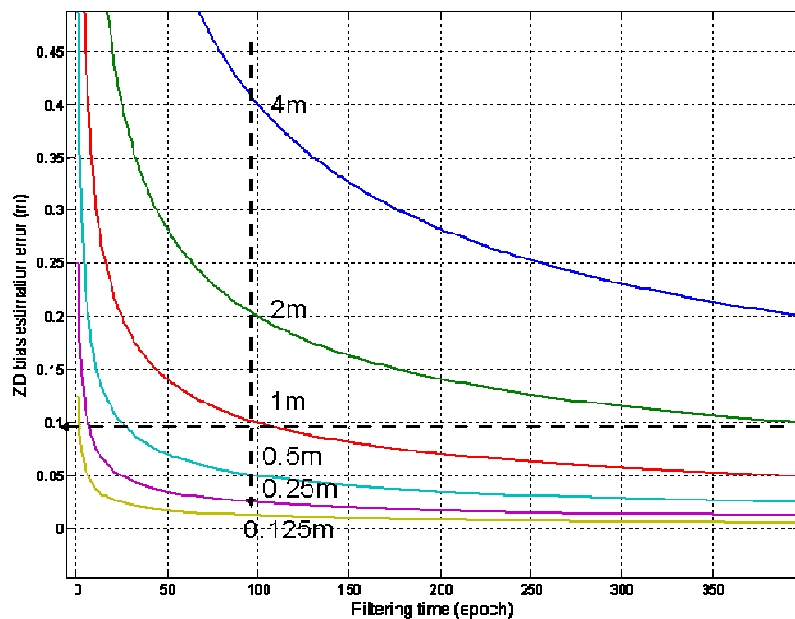


Fig 6. Illustration of the convergence of various magnitudes of the initial ZD phase bias errors (single epoch) versus the filtering time (epochs) under zero mean and white noise conditions.

5. Conclusions

Use of multiple-frequency GNSS signals can potentially redefine future CORS network-based services on both a regional and global basis. GNSS reference stations equipped with triple-frequency GNSS receivers may be spaced up to a few hundred kilometres apart, supporting many types of services or applications, including: network-based real-time kinematic positioning, satellite clock estimations, precise point positioning, regional integrity determination, zenith tropospheric delay estimation, and ionospheric total electron content mapping. However, all these network-based services depend on two fundamental types of measurements: (1) ambiguity-resolved double-differenced (DD) phase measurements, and (2) phase bias calibrated zero-differenced (ZD) phase measurements. This paper has described generalised, network-based geometry-free models for three carrier ambiguity resolution (TCAR) and phase bias estimation with DD and ZD code and phase measurements, respectively.

The general geometry-free TCAR models for DD phase measurements were formed with two EWL/WL virtual signals, to allow for very rapid and reliable ambiguity resolution for DD phase measurements over baseline lengths of hundreds of kilometres, and one additional ML or NL signal for AR over the longer periods, e.g., minutes to ten, all through the simplest averaging and rounding processes. This finding is profound for CORS network-based services, where use of continuous observations is never a problem, but the inter-station distances matter a lot. In addition to the traditional rounding process that all the geometry-free TCAR methods can use, the paper has also introduced a more general network-based geometry-free model, where all the DD ambiguities are more rigorously resolved using the LAMBDA method.

Geometry-free models for calibration of three carrier phase biases of ZD phase measurements have been similarly established for selected virtual signals. Both carrier phase ambiguity resolution and phase bias estimation problems are formulated together on a network basis in order to improve phase bias estimation accuracy. The resolved DD integer ambiguities between stations provide constraints for ZD phase bias calibration, whereas better calibrated ZD phase biases can lead to reliable DD phase ambiguity determination. Precisely calibrated ZD phase measurements and ambiguity-resolved DD phase measurements can be obtained over a local or regional CORS network to support various GNSS applications.

Numerical analyses have concluded that single epoch integer estimation for the first best EWLs will achieve success rates of greater than 98%, which can be improved to 100% by averaging over several epochs. AR of the second selected EWL/WL signal does not provide AR success rates as high as the first EWL, but still performs significantly better than that of the WL signal $\phi_{(1,-1,0)}$ often used in other TCAR methods. Results from numerical experiments with 24-hour dual-frequency GPS data from three US CORS stations, with separations of 21km, 56km and 74km, have demonstrated the consistency between the theoretical predictions and actual AR success rates of the proposed models, based on the STDs assumed or obtained from the real data sets. Results have also confirmed that with the LAMBDA procedure the geometry-free AR success rates can be improved only slightly compared to rounding the float solution to the nearest integers. By introducing DD constraints between three stations and eight satellites, the accuracy of phase bias estimates of ZD measurements is improved by a factor of 1.4, demonstrating the performance potential of the network-based method for precise GNSS real time applications.

Acknowledgements

This work was carried out with financial support from the Cooperative Research Centre for Spatial Information (CRCSI) project 1.4:- “Delivering precise positioning services in regional areas”, 2007-2010.

References

- Cislowski G, Higgins MB (2006), SunPOZ: Enabling Centimetre Accuracy GNSS Applications in Queensland, Paper 100, Proceedings of IGNSS 2006 Symposium on GPS/GNSS, July, Gold Coast, Australia.
- De Jonge PJ, Teunissen PJG, Jonkman NF, Joosten P (2000), The Distributional Dependence of the Range on Triple Frequency GPS Ambiguity Resolution, Proceedings of ION-NTM 2000. pp 605-612, Jan 26-28, Anaheim, CA.
- Feng Y (2008), GNSS Three Carrier Ambiguity Resolution Using Ionosphere-reduced Virtual Signals, Journal of Geodesy, <http://dx.doi.org/10.1007/s00190-008-0209-x>.

Feng Y, Rizos C (2005), Three Carrier Approaches for Future Global, Regional and Local GNSS Positioning Services: Concepts and Performance Perspectives, Proceedings of ION-GNSS 2005, pp 2277-2787, Sept 13-16, Long Beach, CA.

Feng Y, Moody M (2006), Improved Phase Ambiguity Resolution Using Three GNSS Signals, PCT/AU2006/000492, <http://www.wipo.int/pctdb>, April.

Feng Y, C Rizos (2007), Geometry-based TCAR Models and Performance Analysis, accepted for publication in IAG Symp. Vol.133, Springer-Verlag.

Feng Y, Rizos C, Higgins M (2007), Multiple Carrier Ambiguity Resolutions and Performance Benefits for RTK and PPP in Regional Areas, Proceedings of ION-GNSS 2007, pp 668-678, Sept 25-28, Fort Worth, TX.

Feng Y, Wang J (2007), Exploring GNSS RTK Performance Benefits with GPS and Virtual Galileo Measurements, Proceedings of ION-NTM 2007, pp 218-226, Jan 22-24, San Diego, CA.

Forsell B, Martin-Neira M, Harris RA (1997), Carrier Phase Ambiguity Resolution in GNSS-2. Proceedings of ION-GPS 1997, pp 1727-1736, Sept 16-19, Kansas City, MO.

Han S, Rizos C (1999), The Impact of Two Additional Civilian GPS Frequencies on Ambiguity Resolutions Strategies, Proceedings of ION Annual Technical Meeting, pp 315-321, June 28-30, Cambridge, MA.

Hatch RR, Jung J, Enge P, Pervan B (2000), Civilian GPS: The Benefits of Three Frequencies, GPS Solutions, Vol 3, No 4, pp 1-9.

Hatch RR (2006), A New Three-Frequency, Geometry-Free Technique for Ambiguity Resolution, Proceedings of ION-GNSS 2006, pp 309-316, Sept 26-29, Fort Worth, TX.

Higgins M.B (2002), Australia's Changing Surveying Infrastructure from Marks in the Ground to Virtual Reference Stations, XXII FIG International Congress, International Federation of Surveyors (FIG), 19-26 April, Washington, DC.

Rizos C., Han S (2003), Reference Station Network Based RTK Systems - Concepts & Progress, *Wuhan University Journal of Nature Sciences*, 8(2B), pp 566-574.

Vollath U, Birnbach S, Landau H (1998), Analysis of Three Carrier Ambiguity Resolution (TCAR) Technique for Precise Relative Positioning in GNSS-2, Proceedings of ION-GPS 1998, pp 417-426, 15 - 18, September 1998, Nashville, TN

Vollath U (2004), The Factorized Multi-Carrier Ambiguity Resolution (FAMCAR) Approach for Efficient Carrier-Phase Ambiguity Estimation, Proceedings of ION-GNSS 2004, pp 2499-2508, Sept 21-24, Long Beach, CA.

Appendix A. Summary of characteristics of useful EWL/WL signals for geometry-free TCAR models ($\beta_{(l,m,n)} \equiv \beta_{(1,1,0)}$)

			$f_{(i,j,k)}$	$\lambda_{(i,j,k)}$	$\beta_{(i,j,k)}$	$\mu_{(i,j,k)}$	Total Noise Level σ_{TN}		
			GHz	metre	-	-	$\sigma_{\delta l}=40\text{cm}$ $\sigma_{\phi 1}=1\text{cm}$ $\sigma_{P 1}=60\text{cm}$	$\sigma_{\delta l}=60\text{cm}$ $\sigma_{\phi 1}=1\text{cm}$ $\sigma_{P 1}=60\text{cm}$	$\sigma_{\delta l}=100\text{cm}$ $\sigma_{\phi 1}=1\text{cm}$ $\sigma_{P 1}=60\text{cm}$
i	j	k					cycle	cycle	cycle
L1	L2	L5	GPS		$\beta_{(1,1,0)}=-1.2833^*$				
0	1	-1	0.0512	5.861	-1.7186	33.2415	0.0961	0.1017	0.1178
1	-6	5	0.0921	3.2561	-0.0744	103.8007	0.3746	0.4097	0.5061
1	-5	4	0.1432	2.0932	-0.6616	55.1119	0.3517	0.3759	0.4447
1	-4	3	0.1944	1.5424	-0.9397	32.1501	0.3543	0.3681	0.4089
1	-3	2	0.2455	1.2211	-1.102	18.9213	0.3819	0.3876	0.4054
1	-1	0	0.3478	0.8619	-1.2833	5.7422	0.4918	0.4918	0.4918
1	0	-1	0.399	0.7514	-1.3391	4.9282	0.5636	0.5645	0.5677
L1	E6	E5a	Galileo		$\beta_{(1,1,0)}=-1.2320$				
0	1	-1	0.1023	2.9305	-1.6498	16.9853	0.1648	0.1767	0.2103
1	-3	2	0.0921	3.2561	-0.3035	51.7879	0.2344	0.2668	0.3511
1	-2	1	0.1944	1.5424	-1.0121	16.597	0.2983	0.305	0.3257
1	-1	0	0.2967	1.0105	-1.232	6.8395	0.4211	0.4211	0.4211
1	0	-1	0.399	0.7514	-1.3391	4.9282	0.5657	0.5692	0.5806
L1	E6	E5b	Galileo		$\beta_{(1,1,0)}=-1.2320$				
0	1	-1	0.0716	4.1865	-1.6079	24.5569	0.1216	0.1281	0.1469
1	-4	3	0.0818	3.6632	-0.2454	78.9612	0.2669	0.2928	0.3635
1	-3	2	0.1535	1.9537	-0.8812	31.2721	0.2775	0.2889	0.3226
1	-2	1	0.2251	1.3321	-1.1124	14.384	0.3352	0.3376	0.3452
1	-1	0	0.2967	1.0105	-1.232	6.8395	0.4211	0.4211	0.4211
1	0	-1	0.3683	0.814	-1.3051	5.3892	0.5214	0.523	0.5279
E1	E6	E5b	Compass		$\beta_{(1,1,0)}=-1.2532$				
0	1	-1	0.0614	4.8842	-1.6504	28.5287	0.1089	0.1148	0.132
1	-5	4	0.0757	3.9602	0.035	107.3736	0.3189	0.3505	0.4366
1	-4	3	0.1371	2.187	-0.7197	46.9308	0.3041	0.323	0.3774
1	-3	2	0.1985	1.5106	-1.0075	24.0799	0.327	0.335	0.3594
1	-1	0	0.3212	0.9333	-1.2532	6.3315	0.4551	0.4551	0.4551
1	0	-1	0.3826	0.7836	-1.3169	5.2172	0.5411	0.5423	0.5462
E2	E6	E5b	Compass		$\beta_{(1,1,0)}=-1.2306$				
0	1	-1	0.0614	4.8842	-1.5915	28.5287	0.1081	0.113	0.1275
1	-5	4	0.0471	6.3707	0.6521	172.6135	0.3029	0.3305	0.4063
1	-4	3	0.1084	2.7646	-0.6179	59.2629	0.2773	0.2945	0.3437
1	-3	2	0.1698	1.7654	-0.9698	28.0859	0.2922	0.2996	0.3221
1	-2	1	0.2312	1.2967	-1.1348	13.9022	0.3425	0.344	0.3491
1	-1	0	0.2926	1.0247	-1.2306	6.8751	0.4153	0.4153	0.4153
1	0	-1	0.354	0.847	-1.2932	5.5752	0.5011	0.5022	0.5057

* Choices of other $\beta_{(l,m,n)}$ may lead to slightly different total noise level (in cycles), but the conclusions on the selection of best virtual signals would remain essentially the same.